Supplementary methods

EV characterisation

The STEV preparations have been extensively characterised in our laboratory by flow cytometry, fluorescence NTA, immunoblotting and functional assays (7, 15). The STEV were further analysed by TEM with anti-placental alkaline phosphatase (NDOG2, in house antibody) and10 nm colloidal gold (Fig S1). We have previously shown that plasma and platelet derived platelets isolated by centrifugation at 20,000 – 30,000 g produce morphologically intact EV of which >95% label positively using an amphoteric membrane specific dye (Cellmask, Invitrogen, CA) by fluorescence NTA (2, 16). Membrane specific staining of neuroblastoma EV and urinary EV was performed using the same protocol.

Initial RICalculator model

Before implementing the Monte Carlo method in RICalculator, a fixed-sampling approach was used. A regular grid of points projected on the aperture was sampled. Initially, samples were only taken along a longitudinal line, fixing polarization to one value across the whole aperture. A weighting factor was used to account for the variation in the width of the aperture circle along this latitude line. However, there were a number of issues with this approach: the weighing of the samples was flawed, using straight-line rather than great-circle distances; the weighting should also be based on the area represented by the sample rather than the width of the aperture. Sampling across each latitudinal line to account for polarization was also introduced.

The modular design of RICalculator made it simple to incorporate the required changes, however the complexity and size of the code was increased significantly by fixes and fixes upon fixes. Concerned that the fixed sampling model might lead to bias towards oversampled areas of the light cone, that it would be hard to quantify the uncertainty of the result, and that it was insufficiently flexible, the fixed sampling method was abandoned in favour of a Monte Carlo model.

The Monte Carlo technique, was first utilized on early computers in the late 40s and has found widespread use in numerical analysis; especially where the sample space is large or calculating exact solutions is complex or impossible. Rather than an ordered pattern of samples, random rays within the cone of light scattered from the particle to the microscope are chosen. This makes finding the angle and polarization of these rays trivial, and as the samples are random and uniformly distributed there is less risk of method bias. The accuracy of Monte Carlo methods was traded against computational effort by varying the number of samples used. Error is proportional to the inverse of the square root of the number of samples, so quadrupling number of samples doubles accuracy. The number of samples to be used was chosen with consideration of calculation time and accuracy; 2000 random rays are used, giving a coefficient of variance (CV) of the model intensity of around 0.23% for 100nm polystyrene nanospheres in water.

Numerical Aperture Determination

Initially, the numerical aperture (NA) of the system was set at 0.4, based on the stated value for the objective lens. However, the possibility that this might not reflect the NA of the system was considered, and RI distributions were analysed under a variety of assumed NA values. These had some impact on mean and modal RI, as well as average error from the nominal RI. No peaks or sharp changes in error or summary statistics were found when NA was varied between 0.1 to 0.5.

The parameters known to be related to NA in microscope systems were investigated, and the diameter of the airy disc and diffraction rings were determined by the wavelength and numerical aperture of the system. The diameter of the airy disc is the limiting factor in resolution of imaging systems, and the relationship is widely discussed in texts on microscopy, astronomy and optics. Numerical aperture is given by $\lambda x / \pi d$, where x is the diameter of a diffraction feature (eg the airy disc or rings), and d is the diameter of that feature in the image plane. The first airy ring maxima was chosen because of the ease of identification, and has a diameter of 1.635π.

Still frames were chosen from two videos of 200nm polystyrene particles at random, and selected if they contained at least five particles with airy diffraction rings. Airy ring diameter was taken as the average of the width and height of boxes visually fitted to the maxima of the rings. The average diameter was 22.71px (22.04-23.39, 95% CI, n=26), corresponding to an NA of 0.21 (0.205 – 0.218, 95% CI), based on a calibration factor of 138nm/px listed for the NS500 instrument used in the NTA software. Based on this finding, an NA of 0.21 was used for RI determination.

Model Validation

The Monte Carlo scattering model used in RICalculator was validated in three ways: by comparison with existing Mie scattering codes; by comparison with results obtained by NTA for particle standards; and through review of the code. Results from RICalculator were compared with the output from Scattnlay, which has been validated against other Mie scattering codes and experimental systems by its authors (8). Narrow-angle scattering, which approximates single-ray scattering, and wide-angle scattering, which approximates scattering efficiency (Qsca), was used for comparison.

Narrow-angle scattering was evaluated for 100nm polystyrene particles in water, with incident 405nm light at polarizations of 0, 45 and 90 degrees, to produce data series linking observer angle and LSI. An angular aperture of 1x10-3 was chosen to approximate single ray scattering. For comparison, scattering parameters were calculated using Scattnlay and used to calculate LSI at these polarizations. Data produced by RICalculator and Scattnlay were found to correspond almost perfectly; combined variance in the normalized ratio was 0.023% for all three polarization angles, with maximal variation around 0.51%. Linear scaling between the two data is completely described by the aperture scaling function in the RICalculator program; to account for increased light collection by larger apertures, RICalculator applies a multiplier based on the aperture size.

Wide-angle scattering can be used to calculate Qsca through the relationships:

〖(1) CSA〗_sca=(∑sca)/I_0 (2) Q_sca=〖CSA〗_sca/〖CSA〗_geo

Where ∑sca is light energy scattered at all angles (determined by wide-angle scattering modelled by RICalculator with an angular aperture of 180 degrees), I0 is incident light intensity (energy per area), CSAsca is scattering cross-sectional area, and CSAgeo is geometric cross-sectional area. Qsca is a unitless ratio of geometric and scattering cross-sections, and may be greater than one for particles with dimensions similar to the wavelength of the incident light. I0 was determined to be π-1, and using these equations Qsca was determined using RICalculator for polystyrene particles in water with 405nm light and particle diameters between 1nm and 5,000nm. The ratio between the values

produced by RICalculator and Scattnlay was found to average unity, and appears normally distributed, although the standard deviation increases with particle diameter.

RICalculator was compared to reference nanospheres observed by NTA. The mean particle diameter obtained under sizing-optimised measurement conditions was taken as the mean particle size of each nanosphere population, and the mean rLSI obtained by NTA under rLSI-optimised measurement conditions described above was taken as the population rLSI. These values conformed well to projected LSI values for silica and polystyrene nanospheres.

Supplementary results

The STEV demonstrated membrane bound structures which labelled positively for placental alkaline phosphatase (Fig S1) and no obvious large protein aggregates. Similarly, urinary EV also demonstrated membrane bound vesicular morphology (Fig S2). Neuroblastoma EV and urinary EV both demonstrated >95% positivity with a membrane specific dye (Fig S3).

Supplementary data

Figure legends

Fig S1. Transmission EM image of STEV labelled with anti-placental alkaline phosphatase by immunogold staining.

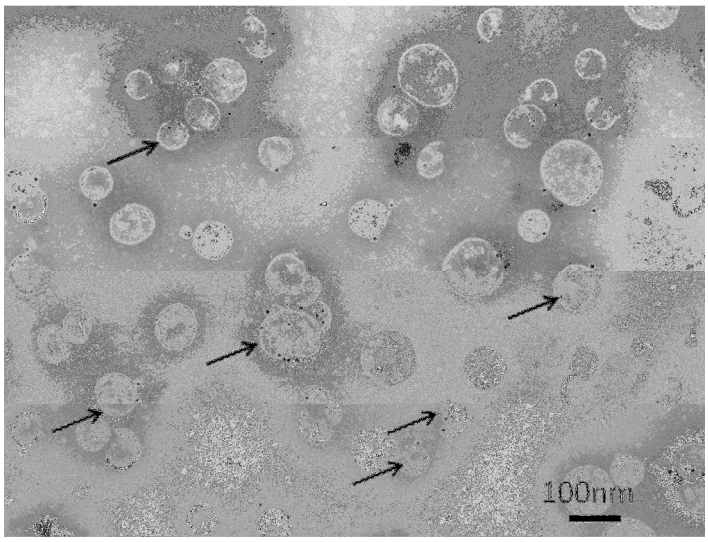

Fig S2. Transmission EM image of freshly isolated urinary vesicles.

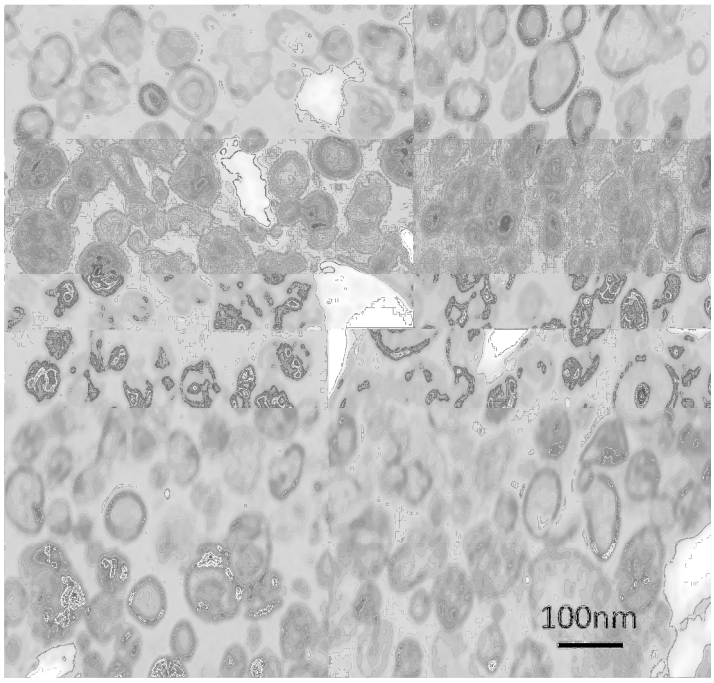

Figure S3. Fluorescent labelling of A) neuroblastoma EV B) urinary EV with a amphoteric membrane-specific dye